TWO–INPUT EPICYCLIC–TYPE TRANSMISSION TRAINS WITH APPLICATION TO TANDEM BICYCLING

Essam Lauibi Esmail
Technical Institute of Diwaniya,
Diwaniya, Iraq

Shaker Sakran Hassan
Associated Professor of Mechanical Engineering
University of Technology, Baghdad, Iraq

Abstract

This paper presents a unification of kinematic and torque balance methods for the analysis of two-input epicyclic-type transmission trains. A method for the derivation of the velocity ratio of an epicyclic gear train in a symbolic form is developed. A single kinematic equation is derived to study the kinematic characteristics of fundamental gear entities. The method relies on previous work on graph theory. It improves on existing techniques used for automatic transmission mechanisms in its ability to accurately solve the kinematics of geared mechanisms and estimating their velocity ratios and arranging them in a descending order in a simpler manner. The results are then used for assignment of the various links of a given two-input epicyclic gear mechanism. This study contributes to the development of a systematic methodology for the torque and power flow analyses of two-input epicyclic gear mechanisms with a reaction link, based upon the concept of fundamental circuit. Specifically, this study presents for the first time a complete design and analysis of two-input velocity changer to be used as a power coupling in a new generation of tandem bicycles. Two new designs are demonstrated.

KEYWORDS: **Epicyclic gear train, Kinematics, Power-flow, Tandem bicycle, Transmission, Two-input, Velocity ratio.**

آليات نقل الحركة ألترسيه ألكوكبيه ثنائية المدخل واستخدامها في الدراجات الهوائية ذات الراكبين

عصام العيبي إسماعيل
مدرس
المعهد التقني ألديوانيه

شاكر سكران حسن
أستاذ مساعد
ألجامعه التكنولوجية

الخلاصه

يقدم هذا البحث طرائق توحيدية لتوازن العزم وكينماتيكيا المجموعات ألترسيه ألكوكبيه ثنائية المدخل. وفيه تم أقتراح طريقــه لاشتقاق النسب السرعيه للمسلسلات ألكوكبيه حيث تم اشتقاق معادله كينماتيكيه واحده لدراسة السمات الكينماتيكيــه للوحــدات البنائيه ألترسيه الاساسيه. وتعتمد ألطريقه على عمل سابق في نظرية المخططات حيث تساهم في تحسين التقنيــات الموجــودة والمستخدمه في دراسة آليات نقل الحركة الآلية في قدرتها على الحل الدقيق لكينماتيكيا الآليات ألترسيه وتخمين نسبها السرعيه وترتيبها تنازليا" بطريقه بسيطة. تهدف النتائج المستحصله إلى تحديد وظيفة الصلات المختلفة لأليــه ترســيه كوكبيــه ثنائيــة المدخل. تساهم هذه الدر اسه في تطوير طريقه منهجيه لتحليل العزوم وتدفق ألقدره خلال آليات نقل الحركة ألترسيه ألكوكبيــه

ثنائية المدخل والتي تحتوي على صلات أرتداديه، بالاعتماد على مفهوم الدائرة الاساسيه. وبشكل خاص تقدم هــذه الدراســه تصميما" وتحليلا" كاملين لمبدل سرعي ثنائي المدخل لاستخدامه في قرن وتوحيد ألقدره في جيل جديد من الدراجات الهوائيــة ثنائية الراكب. ولإيضاح ألطريقه عمليا" فقد تم تبيانها تفصيلا" في تصميمين جديدين.

Nomenclature

EGM	Epicyclic gear mechanism
EGT	Epicyclic gear train
FC_k	k^{th} Fundamental circuit
FGE	Fundamental gear entity
$N_{p,x}$	Gear ratio defined by a planet gear *p* with respect to a sun or ring gear *x*. $N_{p,x} = \pm Z_p / Z_x$, where Z_p and Z_x denote the numbers of teeth on the planet and the sun or ring gear, respectively, and the positive or negative signs depends on whether *x* is a ring or sun gear.
$R^{z}_{x,y}$ Or e	Velocity ratio between links *x* and *y* with reference to link *z*
$T_{ga,k}$, $T_{gb,k}$ and $T_{c,k}$ Or *Ti*	External torques exerted on links *ga, gb* and *c* of the k^{th} Fundamental circuit or exerted on link *i*
Two-dof	Two-degree of freedom
Zi	Number of teeth on gear *i*
c	Carrier
ga	Gear a
gb	Gear b
p	Planet gear
r	Ring gear
s	Sun gear
ω_i	Angular velocity of link *i*

Introduction

A literature survey reveals that numerous methodologies have been proposed for the kinematic analysis of epicyclic gear trains [1, 9, 14, 15, 18 and 23]. Using graph theory, (Buchsbaum and Freudenstein, 1970) investigated the structural characteristics associated with epicyclic gear trains (EGTs) and proposed a systematic methodology for the structural synthesis of such mechanisms. Subsequently, (Freudenstein, 1971) proposed a systematic methodology for the kinematic analysis of EGTs. Freudenstein's method utilizes the concept of fundamental circuits which can be readily derived from the graph of an EGT. The method was elaborated in more detail by (Freudenstein and Yang, 1972). Conventionally, the analysis is performed manually. Recently, there has been an increasing interest in the development of computer aided analysis programs [4, 16]. The concept of fundamental circuit was further extended to force and power flow analysis for EGTs by other researchers [19, 20 and 22]. (Hsieh and Tsai, 1996b) apply similar formulations in conjunction with their kinematic study (1996a) to determine the most efficiency kinematic configuration of one-degree of freedom automatic transmission mechanisms (Hsieh and Tsai, 1998).
The concept of fundamental circuit is a powerful tool for automated analysis of EGTs. However, the analysis involves the solution of a set of linear equations for all the kinematic variables. The area that attracted little attention is the two-dof EGTs. (Corey, 2003) attempted to present a solution technique for finding a total speed and force solution to two-dof EGTs in the most general case possible. Unfortunately, he got confused between the rotational speeds and torques of EGTs in the general case

and those of specific cases, which render those solution techniques physically meaningless (Esmail, 2007).

(Mir-Nasiri and Hussaini, 2005) had presented a new concept of mobile robot speed control by using two degree of freedom gear transmission made up of a basic EGT. A basic EGT consists of a sun gear, a ring gear, and a carrier as shown in **Figure 1.**

The first step in the design process of two-input mechanisms involves finding the configuration that not only provides the correct speed ratios, but also meets other dynamic and kinematic requirements. In general, in order to create a physical model of the system, all relevant physical relations such as speed, torque and power flow must be examined. The absence of torque and power flow analyses have led to flawed simulation results in (Mir-Nasiri and Hussaini, 2005).

The present paper applies the concepts of fundamental circuits and fundamental gear entities (FGEs) for the kinematic and dynamic analyses of two-input EGTs. A single kinematic equation is derived to study the kinematic characteristics of FGEs. The results are then used for the estimation and comparison of various velocity ratios of an epicyclic gear mechanism , which lead to the development of a more efficient methodology for the assignment of the various links of a given two-input epicyclic gear mechanism.

Specifically, this study presents for the first time a complete design of two-input velocity changer to be used as a power coupling in a new generation of tandem bicycles.

In what follows, the concepts of fundamental circuit and fundamental gear entity will be reviewed.

Fundamental Circuit

The fundamental circuit is defined as a circuit consisting of one geared edge and several turning pair edges connecting the endpoints of the geared edges (Buchsbaum and Freudenstein, 1970). **Figure 2** (a) shows a gear pair which consists of two gears, *ga* and *gb*, and a supporting carrier, *c*. **Figure 2** (b) shows the corresponding schematic representation, which is a fundamental circuit. This schematic diagram consists of a block, three nodes, and three chords. The block represents a fundamental circuit. The symbol FC_k denotes the k^{th} fundamental circuit of an EGT. The nodes represent the links of the fundamental circuit which transfer power or torque to the other fundamental circuits. The chords connecting the nodes to the block are labeled with $T_{ga,k}$, $T_{gb,k}$ and $T_{c,k}$ which denote the external torques exerted on links *ga*, *gb*, and *c*.

Fundamental Gear Entity

(Chatterjee and Tsai, 1995) defined the fundamental geared entity (FGE) as a mechanism represented by a graph formed by a single second-level vertex or a chain of heavy-edge connected second-level vertices together with all the lower vertices connecting them to the root. **Figure 1** shows the canonical graph of the basic epicyclic gear train shown in the same Figure.

There are two frequently used FGEs, one contains only one planet and the other contains two meshing planets. The graphs and functional schematics of a single-planet FGE and a double-planet FGE are shown in **Figures. 3 and 4**, respectively.

FGEs with more than two meshing planets and/or with multiple compound planets are not practical (Gott, 1991) and will be excluded from this study.

In a single-planet FGE, the coaxial links include a carrier and several first-level gears meshing with one planet gear.

In a double-planet FGE, there are two meshing planets, one carrier, and several coaxial gears meshing with either one of the two planets.

Kinematics of Fges

The velocity relationship among these coaxial links should be established in order to effectively compute the velocity ratios of a transmission mechanism.
The term "gear ratio" is used in this paper to denote the ratio of a meshing gear pair, while the term "velocity ratio" is used to denote the velocity ratio between the input link and the output link of an EGM.

$$N_{p,x} = \pm Z_p / Z_x \tag{1}$$

Considering the kinematics of a fundamental circuit, the fundamental circuit equation can be written as (Buchsbaum and Freudenstein, 1970):

$$(\omega_x - \omega_c)/(\omega_p - \omega_c) = N_{p,x} \tag{2}$$

Equation (2) can be re-written for the coaxial links of the single-planet FGE and the double-planet FGE shown in Figs. 3 and 4 as follows

$$(\omega_i - \omega_c)/(\omega_p - \omega_c) = N_{p,i} \tag{3}$$

$$(\omega_j - \omega_c)/(\omega_p - \omega_c) = N_{p,j} \tag{4}$$

$$(\omega_k - \omega_c)/(\omega_p - \omega_c) = N_{p,k} \tag{5}$$

And

$$(\omega_l - \omega_c)/(\omega_p - \omega_c) = N_{p,l} \tag{6}$$

Dividing Eq. (3) by (4) yields a kinematic equation relating the angular velocities of the two gears *i* and *j*, and the carrier *c*.
Let the symbol $R^c_{i,j}$ denote the velocity ratio between links *i* and *j* with reference to link *c*. That is

$$R^c_{i,j} = \frac{\omega_i - \omega_c}{\omega_j - \omega_c} = \frac{N_{p,i}}{N_{p,j}} \tag{7}$$

The gear ratio for the coaxial gears that are not meshing directly with the planet gear on which the velocity ratio is calculated and are meshing with the other planet gear can be found in terms of the gear ratio of the two planets $(N_{p,p1})$ as

$$N_{p,x} = N_{p,p1} \cdot N_{p1,x} \tag{8}$$

Dividing Eq. (3) by (5) yields

$$R^c_{i,k} = \frac{\omega_i - \omega_c}{\omega_k - \omega_c} = N_{p,i}/N_{p,k} \tag{9}$$

Where; $N_{p,k} = N_{p,p1} \cdot N_{p1,k}$, for the double-planet FGE.

Eliminating ω_p and ω_c from the fundamental circuit equations (3), (4) and (5), yields

$$R_{i,j}^{k} = \frac{\omega_i - \omega_k}{\omega_j - \omega_k} = \frac{N_{p,i} - N_{p,k}}{N_{p,j} - N_{p,k}} \quad (10)$$

Similarly, eliminating ω_p and ω_c from the fundamental circuit equations (3), (5) and (6), yields

$$R_{i,k}^{l} = \frac{\omega_i - \omega_l}{\omega_k - \omega_l} = \frac{N_{p,i} - N_{p,l}}{N_{p,k} - N_{p,l}} \quad (11)$$

Where; $N_{p,l} = N_{p,p1} \,.\, N_{p1,l}$ **,** for the double-planet FGE.
In general we can write

$$R_{x,y}^{z} = \frac{\omega_x - \omega_z}{\omega_y - \omega_z} = \frac{N_{p,x} - N_{p,z}}{N_{p,y} - N_{p,z}} \quad (12)$$

Using the facts that $N_{p,p} = 1$ and $N_{p,c} = 0$, equation (12) provides a basis for the velocity ratio analysis of single-planet and double-planet FGEs and so on. Only this equation can be used to study the kinematic characteristics of all of the FGEs, which makes the kinematic analysis of EGTs very simple.

Velocity Ratio Ranges
Kinematic inversion is defined as the process of selecting the input, output, and fixed links for a mechanism. Given three coaxial links x, y and z the following basic characteristics relate the velocity ratios of these links.

1. $R_{y,x}^{z} = 1 / R_{x,y}^{z}$

2. $R_{x,z}^{y} + R_{x,y}^{z} = 1$

All other velocity ratios of the three links due to kinematic inversions can be found by applying characteristics 1 and 2 as shown in **Table 1.**
The velocity ratio ranges are classified into three kinds; greater than one, between zero and one, or less than zero. Again, by applying the kinematic inversions, the velocity ratio ranges of an EGT can be deduced as shown in Table 1.

<u>Velocity Ratio Relations</u>

A one-degree of freedom EGT giving and taking power from the external environment requires at least an input, an output and a fixed link. Thus, to function effectively it requires at least three ports. Similarly, a two-dof EGT requires at least four ports, and so on. Following a similar procedure to that used by (Hsieh and Tsai, 1996b) with major differences, we can write;
Let $R_{x,o}^{y}$ and $R_{y,o}^{z}$ denote two velocity ratios of an EGT. Dividing $1 - R_{x,o}^{z}$ by $1 - R_{y,o}^{z}$ and after simplification, yields

$$\frac{1-R^{z}_{x,o}}{1-R^{z}_{y,o}} = 1 - R^{y}_{x,o} \tag{13}$$

Dividing $R^{z}_{x,o}$ by $R^{z}_{y,o}$ and after simplification, yields

$$\frac{R^{z}_{x,o}}{R^{z}_{y,o}} = R^{z}_{x,y} \tag{14}$$

Hence if the ranges of $R^{y}_{x,o}$ and $R^{z}_{y,o}$ are known, the velocity ratio relation between $R^{z}_{x,o}$ and $R^{z}_{y,o}$ can be deduced from Eqs. (13) and (14). For example, if $1 > R^{y}_{x,o} > 0$ then

$$1 > \frac{1-R^{z}_{x,o}}{1-R^{z}_{y,o}} > 0 \tag{15}$$

Furthermore, if $0 > R^{z}_{y,o}$ then Eq. (15) can be further simplified to $1 - R^{z}_{y,o} > 1 - R^{z}_{x,o} > 0$. This equation implies that the velocity ratio $R^{z}_{x,o}$ can assume two possible ratio ranges, $0 > R^{z}_{x,o}$, and $1 > R^{z}_{x,o} > 0$. From Eq. (14), if $0 > R^{z}_{x,o}$, then $1 > R^{z}_{x,y} > 0$, and the velocity ratio relations can be deduced as $0 > R^{z}_{x,o} > R^{z}_{y,o}$. Also, if $1 > R^{z}_{x,o} > 0$, then $0 > R^{z}_{x,y}$ and the velocity ratio relations is $1 > R^{z}_{x,o} > 0 > R^{z}_{y,o}$. Twelve velocity ratio relations can be derived from Equations (13) and (14) for any four coaxial links of an EGT as shown in **Table 2**. These velocity ratio relations are three more than the nine relations given in (Hsieh and Tsai, 1996b). This is because that paper has not taken in consideration the effect of $R^{z}_{x,y}$ on the velocity ratio relations.

Procedure for Assignment of Four Coaxial Links of A Two-Dof Egt

Most enumeration procedures are done through the process of generating and testing. The procedure is thus divided into two parts: a generator of all possible solutions and a tester that selects only those solutions that meet the constraints.

An EGT can provide several velocities depending on the assignment of the input, output and fixed links. These various velocities need to be estimated and arranged in a descending order to arrive at a proper design.

Selecting three out of any four coaxial links of an EGT (x, y, z, o) at a time, yields four sets of three coaxial links (x, y, z),(x, y, o),(x, z, o) and (y, z, o). By expressing the train velocity ratios in terms of the gear ratios of its gear pairs with the help of Eq. (12), the velocity ratio ranges can be estimated without knowing the exact dimensions of the epicyclic gear mechanism. Other velocity ratio ranges due to kinematic inversions can be found using **Table 1**.

Furthermore, the velocity ratio ranges are compared with the velocity ratio relations shown in Table 2, to identify all other velocity ratio ranges of the EGT. The results are then used to identify the proper assignment of the links of a two-input epicyclic gear mechanism.

Torque Analysis

Torque Analysis of a Fundamental Circuit

For a fundamental circuit of an EGT, it is well known that under static equilibrium, torques acting on the three links of a fundamental circuit must be summed up to zero:

$$T_{ga,k} + T_{gb,k} + T_{c,k} = 0 \tag{16}$$

It is also well known that under constant-velocity operation and in the absence of friction, the net power passing through a fundamental circuit is zero. Power is the product of torque and angular velocity ($T.\omega$):

$$T_{ga,k} \cdot \omega_{ga} + T_{gb,k} \cdot \omega_{gb} + T_{c,k} \cdot \omega_{c} = 0 \tag{17}$$

Solving Equations (2), (16) and (17), yields:

$$T_{gb,k} + N_{gb,ga} \cdot T_{ga,k} = 0 \tag{18}$$

And

$$T_{c,k} + (1 - N_{gb,ga}) \cdot T_{ga,k} = 0 \tag{19}$$

Equations (18) and (19) express two of the external torques in terms of the third. The word "external" refers to all sources that are external to the gear pair of interest. Thus, external torques come from all the links that are connected to links *ga, gb* and *c*.

Torque Analysis of Two-Input EGTs with a reaction link

Due to the fact that the function of a transmission mechanism is to provide proper torques and velocities for a vehicle, it is essential to identify the relations among the velocity ratio, torque distribution and the power flow in an EGM.

Under steady-state operation, it is well-known that torques exerted on links *x, y, z,* and *o* about the central axis of the EGT are summed to zero; that is

$$T_x + T_y + T_z + T_o = 0 \tag{20}$$

Where *Ti* denotes an external torque exerted on link *i*.

Similarly, it is well-known that the net power flowing into the system via the four coaxial links are summed to zero; that is

$$T_x.\omega_x + T_y.\omega_y + T_z.\omega_z + T_o.\omega_o = 0 \tag{21}$$

Eliminating T_z from Equations (20) and (21) and making use of Eq. (12), and after simplification, yields

$$T_o = -R^{z}_{x,o}.T_x - R^{z}_{y,o}.T_y \tag{22}$$

Similarly, eliminating *To* from Equations (20) and (21) and making use of Eq. (12), yields

$$T_z = (R^{z}_{x,o} - 1).T_x + (R^{z}_{y,o} - 1).T_y \tag{23}$$

Equations (22) and (23) relate torques exerted by links *x, y, z* and *o* in terms of the velocity ratios $R^{z}_{x,o}$ and $R^{z}_{y,o}$.

Each-Link Torque Analysis of Two-Input EGTs

The torque and power equilibrium equations can be written for an n-link EGT as follows:

- First, writing Equations (18) and (19) once for each fundamental circuit will result in 2(n-2) equations.
- Second, at each node, applying the condition that the sum of torques on the link is equal to zero will result in n-node equations. A total of (3n-4) linear equations are obtained which can be written in a compact form by using a matrix-vector notation as

$$[N]_{A\times B}[T]=[T_{in}] \tag{24}$$

Where $[N]_{A\times B}$ is a system of ($A\times B$) matrix whose elements are functions of the gear size ratios (*Ngb,ga*), and $[T]$ denotes the vector of (B) torques. Hence, regardless of which links are assigned as the input, output, or fixed link, Eq. (24) can be used to solve for the (B) unknown torques in terms of the input torques $[T_{in}]$.

These methodologies are perhaps best illustrated through a design example.

Case Studt: Multi-Rider Human Powered Vehicle

Epicyclic gear trains are considered as the most effective method for coupling the relatively inconsistent inputs of two human riders (Corey, 2003). What follows is the design of such a gear train using the present new methodologies. The first step in the design process is to set fourth any design constraints on the design.

Design Constraints

In this paper, several requirements must be met for the design to be viable. These are the same as those in (Corey, 2003):

1. The drivers are to be seated with their backs to one another. This means that at the system's operating point, the two inputs rotate in opposite directions, $\omega i1 / \omega i2 < 0$.
2. The output link moves slightly above the nominal pedal cadence of 80 rpm pedal velocity associated with efficient riding $80 \le |\omega o| \le 120$.
3. Both riders pedal at approximately the same velocity and contribute approximately the same percentage of the output power.

Plan 1

An EGT with one carrier and three coaxial gears meshing with one planet is shown in Fig. 5. Assume that the sizes of the sun gears are in the descending order of gear 2 > gear 1. Selecting three out of the four coaxial links (1, 2, 4, 5) at a time, yields four sets of three coaxial links (1, 2, 4),(1, 5, 4),(2, 5, 4) and (1, 2, 5). For the coaxial links (1, 2, 4), and making use of Eq. (12), the velocity ratio $R^{4}_{1,2}$ can be found as

$$R^{4}_{1,2}=\frac{N_{3^1,1}}{N_{3^2,2}}=\frac{Z_{3^1}\,.\,Z_2}{Z_{3^2}\,.\,Z_1} \tag{25}$$

It can be shown that $R^{4}_{1,2} > 1$.

For the coaxial links (1, 5, 4), and making use of Eq. (12), we can find

$$R_{1,5}^{4} = \frac{N_{3^1,1}}{N_{3^2,5}} = -\frac{Z_{3^1} \cdot Z_5}{Z_{3^2} \cdot Z_1} \tag{26}$$

It is apparent that $0 > R_{1,5}^{4}$. In a similar way, we can find that $0 > R_{2,5}^{4}$ and $R_{1,2}^{5} > 1$. All other velocity ratios and velocity ratio inversions can be found from **Table 1**. These are used to construct Table 3.
To search for an appropriate assignment of the four coaxial links, one can examine, in general the first and second design constraints which can be written in notation consistent with that used in Table 2 as

$$1 > R_{y,o}^{z} > 0 > R_{x,o}^{z} \quad and \quad 0 > R_{x,y}^{z} \tag{27}$$

Where *y* and *o* rotate in the same direction and *x* rotates in the opposite direction.
By searching in Table 3 for the velocity ratio ranges that satisfy Eq. (27), only two possible solutions can be found:

1. $1 > R_{2,1}^{4} > 0 > R_{5,1}^{4}$, which gives $x = 5$, $y = 2$, $o = 1$ and $z = 4$,and
2. $1 > R_{4,5}^{2} > 0 > R_{1,5}^{2}$, which gives $x = 1$, $y = 4$, $o = 5$ and $z = 2$

These two assignments are the potential candidates for achieving a proper design. After establishing a broad range of R-ranges to be considered, the next task is to attempt to apply the design constraints to the governing equations of the system.
Examining the third design constraint, it is convenient to write it in the form

$$T_x \cdot \omega_x = T_y \cdot \omega_y \tag{28}$$

Or

$$\frac{T_x}{T_y} = \frac{\omega_y}{\omega_x} = -1 \tag{29}$$

Obviously, since Eq. (22) must hold for the power contribution from each rider to be equal, and the input torques are equal and opposite, the velocity ratios are related after simplification by

$$R_{x,o}^{z} = -R_{y,o}^{z} \tag{30}$$

And from Eq. (14) and the first and third design constraints, we get

$$R_{x,y}^{z} = -1 \tag{31}$$

Since the human body provides most efficient power at a nominal pedal cadence of 80 rpm pedal velocity associated with efficient riding (Corey, 2003), it would be advantageous to select a gear ratio that would place the absolute value of the output velocity in the range of 120 rpm, as required by the second design constraint. That is

$$R_{y,o}^{z} = 2/3 \tag{32}$$

And

$$R_{x,o}^{z} = -2/3 \tag{33}$$

Applying Eq. (31) to the first potential solution and simplifying, we get

$$R_{5,2}^{4} = -Z_2/Z_5 \tag{34}$$

Since Z_5 is larger than Z_2, and then $R_{5,2}^{4}$ can never be equal to minus unity, which will fail the third design constraint requiring that, the power contribution from each rider to be equal.
Applying Eq. (31) to the second potential solution and simplifying, we get

$$R_{1,4}^{2} = 1 - (Z_{3^1} \cdot Z_2/Z_{3^2} \cdot Z_1) = -1 \tag{35}$$

After more simplification, we get

$$Z_{3^1} \cdot Z_2/Z_{3^2} \cdot Z_1 = 2 \tag{36}$$

Applying Equations (32) and (33) and simplifying, we get

$$R_{4,5}^{2} = Z_5/(Z_2 + Z_5) = 2/3 \tag{37}$$

And

$$R_{1,5}^{2} = \frac{\dfrac{-Z_{3^1}}{Z_1} + \dfrac{Z_{3^2}}{Z_2}}{\dfrac{Z_{3^2}}{Z_5} + \dfrac{Z_{3^2}}{Z_2}} = -2/3 \tag{38}$$

Also, from geometric considerations with all gears having the same diametrical pitch,

$$Z_{3^1} + Z_1 = Z_{3^2} + Z_2 \tag{39}$$

And

$$Z_5 = Z_2 + 2 \,.\, Z_{3^2} \tag{40}$$

The solution of Equations (36), (37), (38), (39) and (40) is listed in Table 4.

Plan 2

This design adopts the compound EGT shown in Fig. 6 to achieve the two-input velocity changer. Assume that the sizes of the sun gears are in the descending order of gear 4 > gear 3^2 > gear 3^1. Selecting three out of the four coaxial links (1, 2, 3, 4) at a time, yields four sets of three coaxial links (1, 2, 3),(2, 3, 4),(1,4,2) and (1, 3, 4). For the coaxial links (1, 2, 3), and since they belong to the same FGE, then making use of Eq. (12), we can find

$$R_{1,2}^{3} = \frac{-N_{5,3^1}}{N_{5,2^1} - N_{5,3^1}} = \frac{Z_5/Z_{3^1}}{(Z_5/Z_{2^1}) + (Z_5/Z_{3^1})} \tag{41}$$

It can be shown that $1 > R_{1,2}^{3} > 0$.

For the coaxial links (2, 3, 4), and since they belong to the same FGE, then making use of Eq. (12), we can find

$$R^4_{2,3} = \frac{Z_{6^2} / Z_4}{(-Z_{6^1} / Z_{3^2}) + (Z_{6^2} / Z_4)} \quad (42)$$

It is apparent that $0 > R^4_{2,3}$.

The velocity ratios of the remaining two sets of three coaxial links can be expressed in terms of the velocity ratios of the above two FGEs. We use the fact that $1 > R^3_{1,2} > 0$ and $0 > R^4_{2,3}$ to begin our evolution. By assigning $x = 1$, $y = 3$, $z = 4$ and $o = 2$ in Table 2, we can write $1 > R^3_{1,2} > 0$ and $0 > R^4_{3,2}$ from kinematic inversions. For this assignment the velocity ratio $R^4_{1,3}$ can assume two possible ratio ranges, $0 > R^4_{1,3}$ and $1 > R^4_{1,3} > 0$. If $0 > R^4_{1,3}$, then $1 > R^4_{1,2} > 0$. Also, if $1 > R^4_{1,3} > 0$ then $0 > R^4_{1,2}$.

Two sets of velocity ratio ranges are possible:

1. $1 > R^3_{1,2} > 0$, $0 > R^4_{2,3}$, $0 > R^4_{1,3}$ and $1 > R^4_{1,2} > 0$, and
2. $1 > R^3_{1,2} > 0$, $0 > R^4_{2,3}$, $1 > R^4_{1,3} > 0$ and $0 > R^4_{1,2}$.

Any assignment of the four coaxial links that gives two known velocity ratios will give similar results. All other velocity ratios can be found from the kinematic inversions of **Table 1**.

Two different tables can be constructed for the above two sets. These are shown in **Tables 5 and 6** (only the first will be considered).

By searching in **Table 5** for the velocity ratio ranges that satisfy Eq. (27), two possible solutions are found:

1. $1 > R^4_{1,2} > 0 > R^4_{3,2}$, which gives x = 3, y = 1, o = 2 and z = 4, and
2. $1 > R^1_{4,3} > 0 > R^1_{2,3}$, which gives x = 2, y = 4, o = 3 and z = 1.

Again, only the first solution will be considered.

Applying Eq. (33) and simplifying, we get

$$R^4_{3,2} = 1 - \frac{Z_{6^1} \cdot Z_4}{Z_{6^2} \cdot Z_{3^2}} = -2/3 \quad (43)$$

After more simplification, we get

$$\frac{Z_{6^1} \cdot Z_4}{Z_{6^2} \cdot Z_{3^2}} = 5/3 \quad (44)$$

Applying Eq. (32), we get

$$R_{1,2}^{4} = 1 - R_{1,4}^{2} = 1 - R_{1,3}^{2} \,.\, R_{3,4}^{2} = 2/3 \quad (45)$$

But

$$R_{3,4}^{2} = 1 - R_{3,2}^{4} = \frac{Z_{6^1} \,.\, Z_4}{Z_{6^2} \,.\, Z_{3^2}} = 5/3 \quad (46)$$

Making use of Eq. (41), we can write

$$R_{1,3}^{2} = 1 - R_{1,2}^{3} = \frac{Z_{3^1}}{Z_{2^1} + Z_{3^1}} \quad (47)$$

Substituting Equations (46) and (47) into Eq. (45), and simplifying, we get

$$Z_{2^1} = 4 \,.\, Z_{3^1} \quad (48)$$

Applying Eq. (31), we get

$$R_{1,3}^{4} = 1 - R_{1,4}^{3} = 1 - R_{1,2}^{3} \,.\, R_{2,4}^{3} = -1 \quad (49)$$

Re-arranging, Eq. (49)

$$R_{1,2}^{3} = \frac{2}{R_{2,4}^{3}} \quad (50)$$

But

$$R_{2,4}^{3} = (R_{3,2}^{4} - 1)/R_{3,2}^{4} = 5/2 \quad (51)$$

And

$$R_{1,2}^{3} = Z_{2^1}/(Z_{2^1} + Z_{3^1}) \quad (52)$$

Substituting Equations (51) and (52) into Eq. (50), and simplifying, we arrive again at Eq. (48). Also, from geometric considerations

$$Z_{6^2} + Z_4 = Z_{6^1} + Z_{3^2} \quad (53)$$

And

$$Z_{2^1} = Z_{3^1} + 2 \,.\, Z_5 \quad (54)$$

The solution of Equations (44), (48), (53) and (54) is listed in Table 7 for $Z_{3^2} = 16$.

Torque and Power-Flow Analysis

The corresponding fundamental-circuit diagram for the EGT shown in Fig. 6 is sketched in **Figure7**. The gear ratios for this train are

$$N_{5,3} = -Z_5/Z_{3^1} = -1.5 \tag{55}$$

$$N_{5,2} = Z_5/Z_{2^1} = 0.375 \tag{56}$$

$$N_{6,3} = -Z_{6^1}/Z_{3^2} = -1 \tag{57}$$

$$N_{6,4} = -Z_{6^2}/Z_4 = -0.6 \tag{58}$$

Writing Eqs (18) and (19) once for each fundamental circuit, yields the following eight linear equations:

$$T_{51} + N_{5,3}.T_{31} = 0 \tag{59}$$

$$T_{11} + (1 - N_{5,3}).T_{31} = 0 \tag{60}$$

$$T_{52} + N_{5,2}.T_{22} = 0 \tag{61}$$

$$T_{12} + (1 - N_{5,2}).T_{22} = 0 \tag{62}$$

$$T_{63} + N_{6,3}.T_{33} = 0 \tag{63}$$

$$T_{23} + (1 - N_{6,3}).T_{33} = 0 \tag{64}$$

$$T_{64} + N_{6,4}.T_{44} = 0 \tag{65}$$

$$T_{24} + (1 - N_{6,4}).T_{44} = 0 \tag{66}$$

Summing all the torques acting on each node to zero, yields the following six linear equations

$$T_{63} + T_{64} = 0 \tag{67}$$

$$T_{31} + T_{33} + T''_{in} = 0 \tag{68}$$

$$T_{51} + T_{52} = 0 \tag{69}$$

$$T_{44} + T_r = 0 \tag{70}$$

$$T_{22} + T_{23} + T_{24} + T_o = 0 \tag{71}$$

$$T_{11} + T_{12} + T'_{in} = 0 \tag{72}$$

Hence, a system of fourteen linear equations is obtained which can be solved for the fourteen unknowns in terms of the first input torque T'_{in} , the second input torque T''_{in} **,** and the gear size ratios. Equations (59) through (72) can be arranged in a matrix form as:

$$\begin{bmatrix} 0 & 0 & 0 & 0 & 0 & 0 & 0 & -0.6 & 0 & 0 & 0 & 1 & 0 & 0 \\ 0 & 0 & 0 & 0 & 1 & 0 & 0 & +1.6 & 0 & 0 & 0 & 0 & 0 & 0 \\ 0 & 0 & 0 & 0 & 0 & 0 & -1 & 0 & 0 & 0 & 1 & 0 & 0 & 0 \\ 0 & 0 & 0 & 1 & 0 & 0 & +2 & 0 & 0 & 0 & 0 & 0 & 0 & 0 \\ 0 & 0 & 0 & 0 & 0 & -1.5 & 0 & 0 & 1 & 0 & 0 & 0 & 0 & 0 \\ 1 & 0 & 0 & 0 & 0 & +2.5 & 0 & 0 & 0 & 0 & 0 & 0 & 0 & 0 \\ 0 & 0 & 0.375 & 0 & 0 & 0 & 0 & 0 & 0 & 1 & 0 & 0 & 0 & 0 \\ 0 & 1 & 0.625 & 0 & 0 & 0 & 0 & 0 & 0 & 0 & 0 & 0 & 0 & 0 \\ 0 & 0 & 0 & 0 & 0 & 0 & 0 & 0 & 0 & 0 & 1 & 1 & 0 & 0 \\ 0 & 0 & 0 & 0 & 0 & 1 & 1 & 0 & 0 & 0 & 0 & 0 & 0 & 0 \\ 0 & 0 & 0 & 0 & 0 & 0 & 0 & 0 & 1 & 1 & 0 & 0 & 0 & 0 \\ 0 & 0 & 0 & 0 & 0 & 0 & 0 & 1 & 0 & 0 & 0 & 0 & 1 & 0 \\ 0 & 0 & 1 & 1 & 1 & 0 & 0 & 0 & 0 & 0 & 0 & 0 & 0 & 1 \\ 1 & 1 & 0 & 0 & 0 & 0 & 0 & 0 & 0 & 0 & 0 & 0 & 0 & 0 \end{bmatrix} \begin{bmatrix} T_{11} \\ T_{12} \\ T_{22} \\ T_{23} \\ T_{24} \\ T_{31} \\ T_{33} \\ T_{44} \\ T_{51} \\ T_{52} \\ T_{63} \\ T_{64} \\ T_r \\ T_o \end{bmatrix} = \begin{bmatrix} 0 \\ 0 \\ 0 \\ 0 \\ 0 \\ 0 \\ 0 \\ 0 \\ 0 \\ -T''_{in} \\ 0 \\ 0 \\ 0 \\ -T'_{in} \end{bmatrix} \tag{73}$$

The solution of Eq. (73) is listed in Table 8. The torque flow through the EGT is shown in Fig. 8. The power-flow through the EGT is shown in Fig. 9.

The second input power transmits through the entire gear train whereas the first input power transmits through links 3, 6 and 2 only. The two riders will supplement each other and a constructive power balance is achieved through the train. Now, it is apparent that the reaction link is used in two-input EGTs to control the direction of rotation of other links and thus the direction of the power-flow.

Conclusions

1. This paper presents a unification of kinematic and torque balance methods for the analysis of two-input epicyclic-type transmission trains.
2. A new method for the derivation of the velocity ratio of EGT in a symbolic form has been developed. A single kinematic equation has been derived to study the kinematic characteristics of FGEs.
3. The results have been used for the estimation and comparison of various velocity ratios of EGMs, which lead to the development of a methodology for the assignment of the various links for a given two-input EGM.
4. Twelve velocity ratio relations have been derived for any four coaxial links of an EGT. These velocity ratio relations are three more than the nine relations given in (Hsieh and Tsai, 1996b). This is because that paper has not taken in consideration the effect of certain velocity ratio ranges on the velocity ratio relations.

5. This study contributes to the development of a systematic methodology for the torque and power flow analyses of two-input epicyclic gear mechanisms (EGMs) with a reaction link, based upon the concept of fundamental circuit. Reaction links are used in two-input EGTs to control the direction of rotation of other links and thus the direction of the power-flow.
6. Specifically, this study has presented for the first time a complete design and analysis of two-input velocity changer to be used as a power coupling in a new generation of tandem bicycles. Two new designs have been demonstrated.

References

[1] Allen, R. R., 1979, "Multi-port Models of the Kinematic and Dynamic Analysis of Gear Power Transmission", ASME J. of Mechanical Design, Volume 101, pp. 258-392.

[2] Buchsbaum, F., and Freudenstein, F., 1970, "Synthesis of Kinematic Structure of Geared Kinematic Chains and Other Mechanisms," Journal of Mechanisms and Machine Theory, Vol. 5, pp. 357-392.

[3] Chatterjee, G., and Tsai, L. W. , 1995, " Enumeration of Epicyclic-Type Transmission Gear Trains, " Transactions of SAE, Vol. 103, Sec. 6, Paper No. 941012, pp. 1415-1426.

[4] Chatterjee, G., and Tsai, L. W., 1996, "Computer-Aided Sketching of Epicyclic-Type Automatic Transmission Gear Trains," Transactions of the ASME, Journal of Mechanical Design,, Vol. 108, No. 3, pp. 405-411.

[5] Corey , C. A., 2003, "Epicyclic gear Train Solution Technique with Application to Tandem Bicycling ," Thesis (M. Sc.) , Department of Mechanical Engineering , Virginia Polytechnic Institute and State University , Blacksburg , VA, USA.

[6] Esmail, E. L., 2007, "Nomographs for Design of Planetary Gear Trains", Accepted for Publication in the Journal of King Abdulaziz University-Engineering Sciences, S. A.

[7] Freudenstein, F., 1971, "An Application of Boolean Algebra to the Motion of Epicyclic Drives," ASME Journal Engineering for Industry, Vol. 93, pp. 176-182.

[8] Freudenstein, F., and Yang, A. T., 1972, "Kinematics and Statics of Coupled Epicyclic Spur Gear Trains", J. of Mechanism and Machine Theory, Volume 7, pp. 263-275.

[9] Gibson, D. and Kramer, S., 1984, "Symbolic Notation and Kinematic Equations of Motion of the Twenty-Two Basic Spur Planetary Gear Trains", ASME J. of Mechanisms, Transmissions and Automation in Design, Volume 106, pp. 333-340.

[10] Gott, P. G., 1991, "Changing Gears," Society of Automotive Engineers, Inc., Warrendale, Pennsylvania.

[11] Hsieh, H. L., and Tsai, L. W., 1996a, "Kinematic Analysis of Epicyclic-Type Transmission Mechanisms Using the Concept of Fundamental Geared Entities", ASME J. of Mechanical Design, Volume 118, pp. 294-299.

[12] Hsieh, H. I., and Tsai, L. W., 1996b,"A Methodology for Enumeration of Clutching Sequences Associated with Epicyclic-Type Automatic Transmission Mechanisms", SAE Transactions, Journal of Passenger Cars, Sec.105, pp. 928-936.

[13] Hsieh, H. L., and Tsai, L. W., 1998, "The Selection of a Most Efficient Clutching Sequence Associated with Automatic Transmission," ASME J. of Mechanical Design, Volume 120, pp. 514-519.

[14] Levai, Z., 1964, "Theory of Epicyclic Gears and Epicyclic Change-Speed Gears", Doctoral Dissertation, Budapest.

[15] Levai, Z., 1968, "Structure and Analysis of Planetary Gear Trains", Journal of Mechanisms, Volume 3, pp. 131-148.

[16] Mruthyunjaya, T.S., and Ravisankar, R., 1985, "Computerized Synthesis of the Structure of Geared Kinematic Chains," Journal of Mechanisms and Machine Theory, Vol. 20, pp. 368-387.

[17] Nazim, M-N. , and Hussaini ,S. , 2005," New Intelligent Transmission Concept for Hybrid Mobile Robot Speed Control ,"Int. J. of Advanced Robotic systems, Volume 2, No. 3, pp, 259-263.

[18] Olson, D. G. , Erdman, A. G. , and Riley, D. R. , 1991, "Topological Analysis of Single-Degree of Freedom Planetary Gear Trains," ASME Journal of Mechanical Design, Vol. 113, pp. 10-16.

[19] Pennestri, E., and Freudenstein, F., 1993, "A Systematic Approach to Power-Flow and Static Force Analysis in Epicyclic Spur-Gear Trains", ASME J. of Mechanical Design, Volume 115, No. 3, pp. 639-644.

[20] Pennestri, E., and Freudenstein, F., 1993, "The Mechanical Efficiency of Epicyclic Gear Trains", ASME Journal of Mechanical Design, Volume 115, No. 3, pp. 645-651.

[21] Smith, D., 1979,"Analysis of Epicyclic Gear Trains via the Vector Loop Approach," Proc. Sixth Applied Mechanisms, Paper No. 10.

[22] Saggora, L. and Olson, D. G., 1992,"A Simplified Approach for Force and Power-Flow Analysis of Compound Epicyclic Spur-Gear Trains," Proc. of the ASME 1992 Design Technical Confs. Advances in Design Automation, DE-Vol. 44-2, Vol. 2, pp. 83-89.

[23] Willis, R. J., 1982, "On the Kinematic of the Closed Epicyclic Differential Gears", ASME J. of Mechanical Design, Volume 104, pp. 712-723.

Table 1: Velocity Ratio Inversions and Ranges.

Velocity Ratios	$R^{z}_{x,y}$	$R^{z}_{y,x}$	$R^{y}_{x,z}$	$R^{y}_{z,x}$	$R^{x}_{y,z}$	$R^{x}_{z,y}$
Velocity Ratio Inversions	e	1/e	1-e	1/(1-e)	(e-1)/e	e/(e-1)
Velocity Ratio Ranges	e>1	1>1/e>0	0>1−e	0>1/(1−e)	1>(e−1)/e>0	e/(e−1)>1
	1>e>0	1/e>1	1>1−e>0	1/(1−e)>1	0>(e−1)/e	0>e/(e−1)
	0>e	0>1/e	1−e>1	1>1/(1−e)>0	(e−1)/e>1	1>e/(e−1)>0

Table 2: Velocity ratio relations for any four coaxial links of an EGT.

$R^{y}_{x,o}>1$	$R^{z}_{y,o}>1$	$1>R^{z}_{x,y}>0$	$R^{z}_{y,o}>1>R^{z}_{x,o}>0$
		$0>R^{z}_{x,y}$	$R^{z}_{y,o}>1>0>R^{z}_{x,o}$
	$1>R^{z}_{y,o}>0$	$R^{z}_{x,y}>1$	$R^{z}_{x,o}>1>R^{z}_{y,o}>0$
	$0>R^{z}_{y,o}$	$0>R^{z}_{x,y}$	$R^{z}_{x,o}>1>0>R^{z}_{y,o}$
$1>R^{y}_{x,o}>0$	$R^{z}_{y,o}>1$	$1>R^{z}_{x,y}>0$	$R^{z}_{y,o}>R^{z}_{x,o}>1$
	$1>R^{z}_{y,o}>0$	$R^{z}_{x,y}>1$	$1>R^{z}_{x,o}>R^{z}_{y,o}>0$
	$0>R^{z}_{y,o}$	$1>R^{z}_{x,y}>0$	$0>R^{z}_{x,o}>R^{z}_{y,o}$
		$0>R^{z}_{x,y}$	$1>R^{z}_{x,o}>0>R^{z}_{y,o}$
$0>R^{y}_{x,o}$	$R^{z}_{y,o}>1$	$R^{z}_{x,y}>1$	$R^{z}_{x,o}>R^{z}_{y,o}>1$
	$1>R^{z}_{y,o}>0$	$1>R^{z}_{x,y}>0$	$1>R^{z}_{y,o}>R^{z}_{x,o}>0$
		$0>R^{z}_{x,y}$	$1>R^{z}_{y,o}>0>R^{z}_{x,o}$
	$0>R^{z}_{y,o}$	$R^{z}_{x,y}>1$	$0>R^{z}_{y,o}>R^{z}_{x,o}$

Table 3: Velocity ratio ranges for the EGT shown in Fig. 5.

$0 > R^{4}_{1,5}$	$0 > R^{4}_{5,1}$	$R^{5}_{1,4} > 1$	$1 > R^{5}_{4,1} > 0$	$R^{1}_{5,4} > 1$	$1 > R^{1}_{4,5} > 0$
$0 > R^{4}_{2,5}$	$0 > R^{4}_{5,2}$	$R^{5}_{2,4} > 1$	$1 > R^{5}_{4,2} > 0$	$R^{2}_{5,4} > 1$	$1 > R^{2}_{4,5} > 0$
$R^{4}_{1,2} > 1$	$1 > R^{4}_{2,1} > 0$	$0 > R^{2}_{1,4}$	$0 > R^{2}_{4,1}$	$1 > R^{1}_{2,4} > 0$	$R^{1}_{4,2} > 1$
$R^{5}_{1,2} > 1$	$1 > R^{5}_{2,1} > 0$	$0 > R^{2}_{1,5}$	$0 > R^{2}_{5,1}$	$1 > R^{1}_{2,5} > 0$	$R^{1}_{5,2} > 1$

Table 4: Number of teeth on the gears of the first design.

$Z_1 = 18\,teeth$	$Z_2 = 24$	$Z_5 = 48$
$Z_{3^1} = 18$	$Z_{3^2} = 12$	

Table 5: First velocity ratio ranges for the compound EGT shown in Fig. 6.

$1 > R^{3}_{1,2} > 0$	$R^{3}_{2,1} > 1$	$1 > R^{2}_{1,3} > 0$	$R^{2}_{3,1} > 1$	$0 > R^{1}_{2,3}$	$0 > R^{1}_{3,2}$
$0 > R^{4}_{2,3}$	$0 > R^{4}_{3,2}$	$R^{3}_{2,4} > 1$	$1 > R^{3}_{4,2} > 0$	$R^{2}_{3,4} > 1$	$1 > R^{2}_{4,3} > 0$
$0 > R^{4}_{1,3}$	$0 > R^{4}_{3,1}$	$R^{3}_{1,4} > 1$	$1 > R^{3}_{4,1} > 0$	$R^{1}_{3,4} > 1$	$1 > R^{1}_{4,3} > 0$
$1 > R^{4}_{1,2} > 0$	$R^{4}_{2,1} > 1$	$1 > R^{2}_{1,4} > 0$	$R^{2}_{4,1} > 1$	$0 > R^{1}_{2,4}$	$0 > R^{1}_{4,2}$

Table 6: Second velocity ratio ranges for the compound EGT shown in Fig. 6.

$1 > R^{3}_{1,2} > 0$	$R^{3}_{2,1} > 1$	$1 > R^{2}_{1,3} > 0$	$R^{2}_{3,1} > 1$	$0 > R^{1}_{2,3}$	$0 > R^{1}_{3,2}$
$0 > R^{4}_{2,3}$	$0 > R^{4}_{3,2}$	$R^{3}_{2,4} > 1$	$1 > R^{3}_{4,2} > 0$	$R^{2}_{3,4} > 1$	$1 > R^{2}_{4,3} > 0$
$1 > R^{4}_{1,3} > 0$	$R^{4}_{3,1} > 1$	$1 > R^{3}_{1,4} > 0$	$R^{3}_{4,1} > 1$	$0 > R^{1}_{3,4}$	$0 > R^{1}_{4,3}$
$0 > R^{4}_{1,2}$	$0 > R^{4}_{2,1}$	$R^{2}_{1,4} > 1$	$1 > R^{2}_{4,1} > 0$	$R^{1}_{2,4} > 1$	$1 > R^{1}_{4,2} > 0$

Table 7: Number of teeth on the gears for the second design.

$Z_{2^1} = 48$	$Z_{3^1} = 12$	$Z_{3^2} = 16$	
$Z_4 = 20$	$Z_5 = 18$	$Z_{6^1} = 16$	$Z_{6^2} = 12$

Table 8: Torque distribution of the EGT shown in Fig. 6 when links 4, 2, 1 and 3 serve as the fixed, output, first input and second input links, respectively.

$T_{11} = -0.5T'_{in}$	$T_{44} = 0.3333\,T'_{in} + 1.6667\,T''_{in}$
$T_{12} = -0.5T'_{in}$	$T_{51} = 0.3T'_{in}$
$T_{22} = 0.8T'_{in}$	$T_{52} = -0.3T'_{in}$
$T_{23} = 0.4T'_{in} + 2T''_{in}$	$T_{63} = -0.2T'_{in} - T''_{in}$
$T_{24} = -0.5333\,T'_{in} - 2.6667\,T''_{in}$	$T_{64} = 0.2T'_{in} + T''_{in}$
$T_{31} = 0.2T'_{in}$	$T_r = -0.3333\,T'_{in} - 1.6667\,T''_{in}$
$T_{33} = -0.2T'_{in} - T''_{in}$	$T_o = -0.6667\,T'_{in} + 0.6667\,T''_{in}$

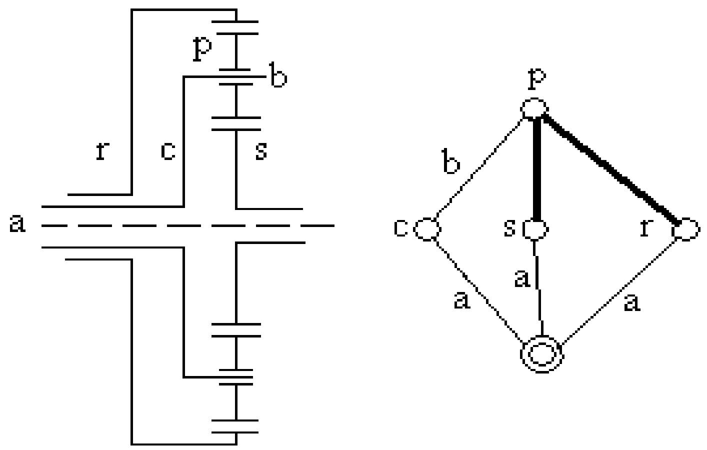

Figure 1: A basic epicyclic gear train with its canonical graph representation.

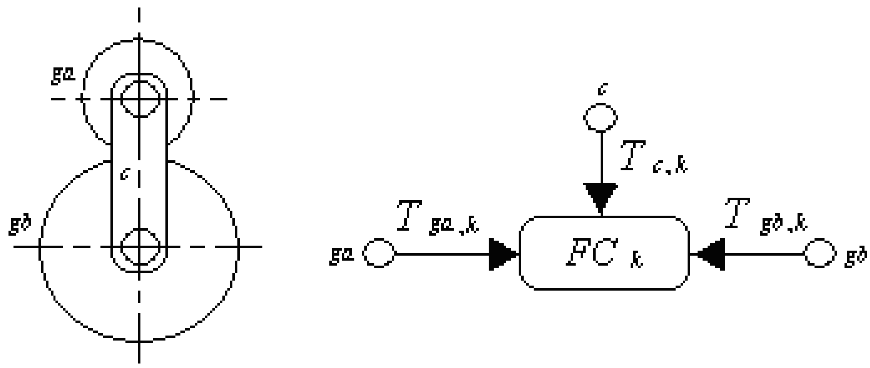

(a) A gear pair. (b) Schematic representation.

Figure 2: A basic gear pair and its schematic representation.

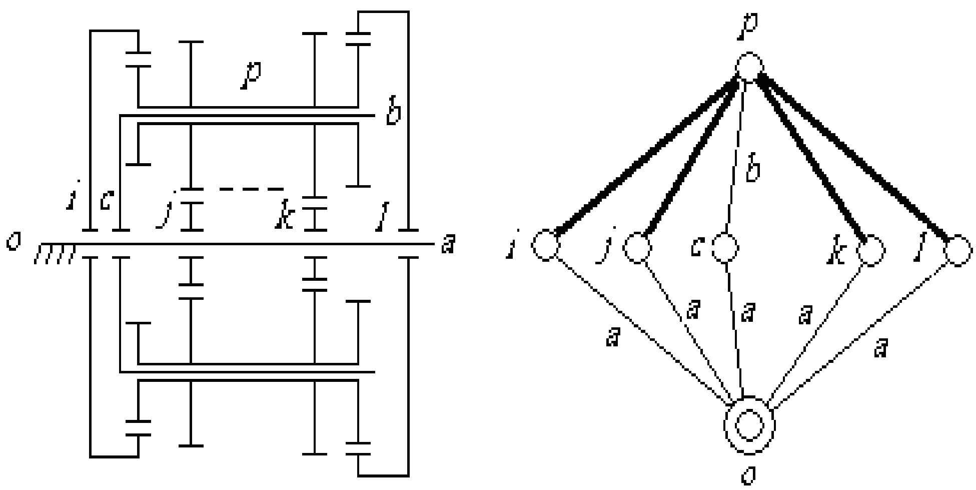

Figure 3: A typical single-planet FGT.

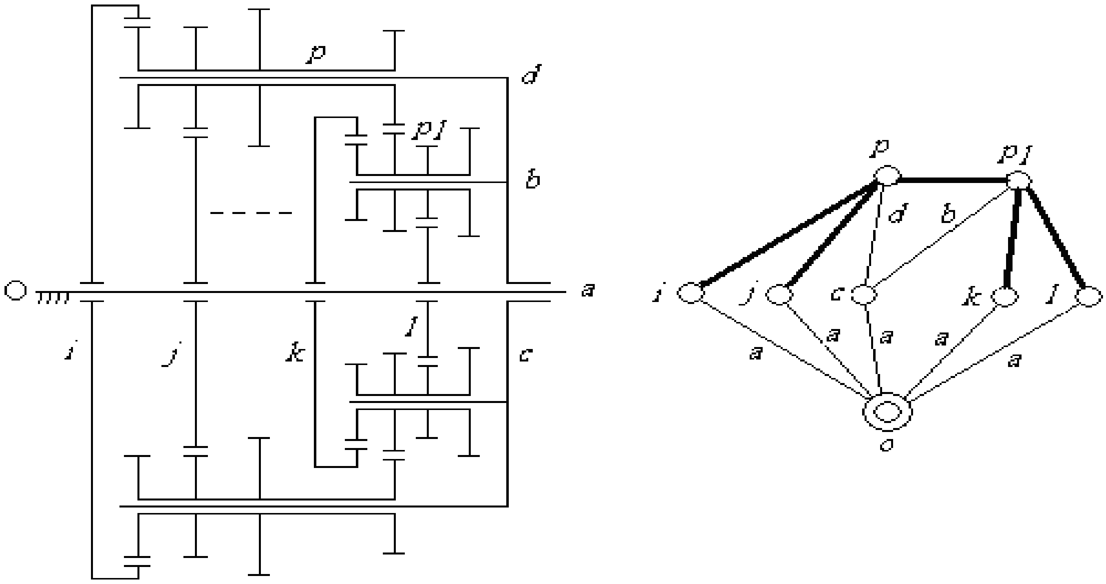

Figure 4: A typical double-planet FGT.

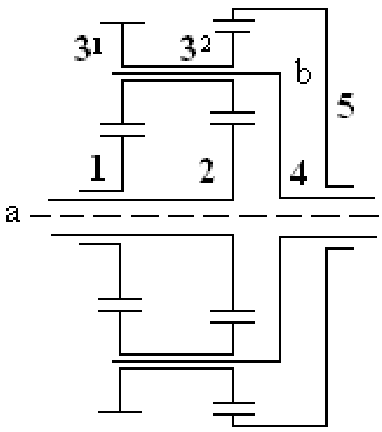

Figure 5: Epicyclic gear train to be used in the first plan.

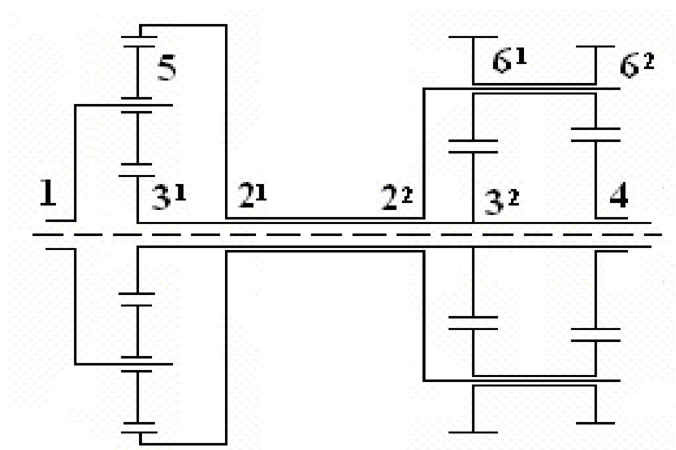

Figure 6: Compound epicyclic gear train to be used in the second plan.

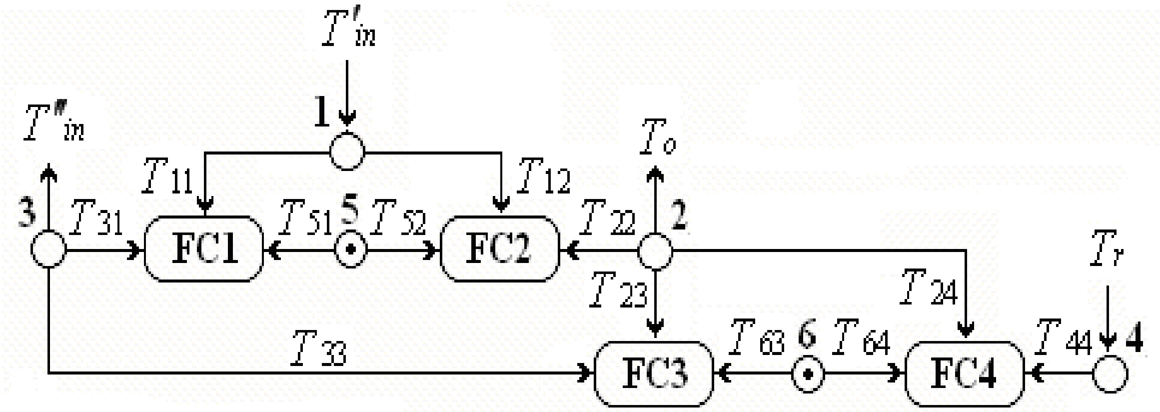

Figure 7: Fundamental-circuit diagram of the EGT shown in Fig. 6 when links 4, 2, 1 and 3 serve as the fixed, output, first input and second input links, respectively.

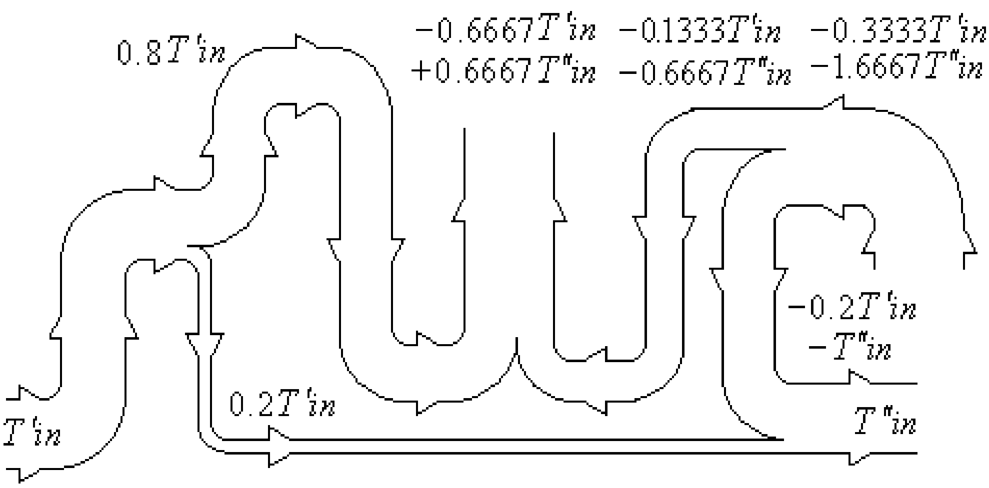

Figure 8: Torque flow through the EGT shown in Fig. 6 when links 4, 2, 1 and 3 serve as the fixed, output, first input and second input links, respectively.

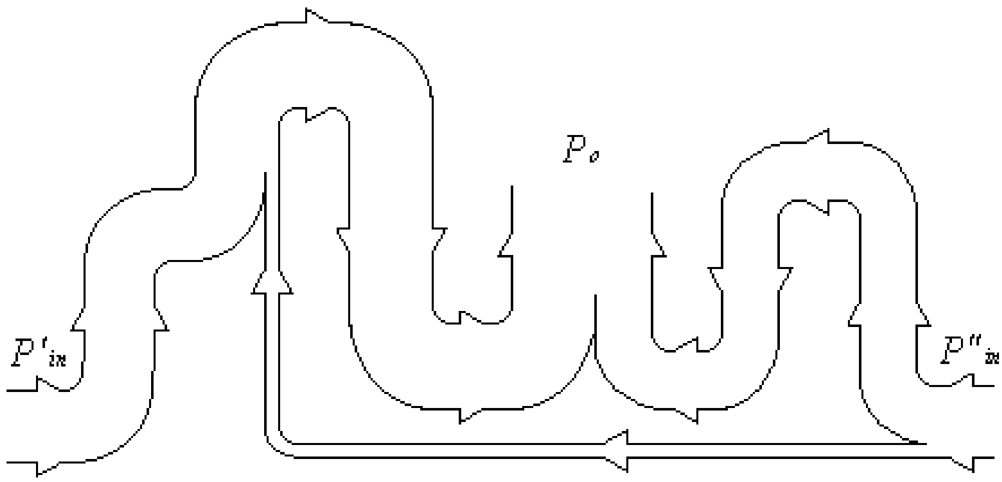

Figure 9: Power- flow through the EGT shown in Fig. 6 when links 4, 2, 1 and 3 serve as the fixed, output, first input and second input links, respectively.